Indonesian Journal of Cancer Chemoprevention, February 2024
ISSN: 2088–0197
e-ISSN: 2355-8989

# Anti-Lung Cancer and Cell Migration Inhibition Properties of Ethyl Acetate Extract of *Selaginella doederleinii* Towards HTB-183 Cells through *In Silico* and *In Vitro* Approach

**Alfiah Amaliyah, Triana Arum Kusumaningtyas, Rifki Febriansah***

School of Pharmacy, Faculty of Medicine and Health Sciences, Universitas Muhammadiyah Yogyakarta, Bantul, Indonesia, 55183

## Abstract

Continuous research and development to obtain novel anti-lung cancer agents is essential, considering the high prevalence and mortality of the disease. The biflavonoid compounds of *Selaginella doederleinii* showed significant anticancer activities. This study aims to determine the cytotoxic and cell migration inhibition properties of ethyl acetate extract of *Selaginella doederleinii* (EAESD) against HTB-183 cells through *in silico* and *in vitro* methods. This study started with extraction and then identified biflavonoids in EAESD by HPLC. *In vitro* analysis was conducted through MTT Assay to observe the cytotoxic properties of EAESD and Wound Scratch Healing Assay to observe its cell migration inhibitory properties. *In silico* studies to obtain the potential anti-lung cancer compounds and their protein targets were conducted through bioinformatics, combining PASS analysis, Swiss Target Prediction, and STITCH. The obtained compounds and protein targets were analyzed in Molecular Docking to evaluate the binding affinities. The result showed that EAESD contained biflavonoid compounds, exhibited cytotoxic activity with an $IC_{50}$ value of 190 µg/ml, and inhibited the migration rate of HTB-183 cells. Based on *in silico* analysis, the three biflavonoids with the highest potential of anti-lung cancer activity along with their target protein are robustaflavone 7,4-dimethyl ether with EGFR, heveaflavone with ESR1, and 7,4',7",4"'-tetra-O-methyl-amentoflavonewith TNF. All compounds can bind to each protein target with the docking score -9.2 kcal/mol, -9.5 kcal/mol, and -6.5 kcal/mol, respectively. This study suggested preliminary data regarding the potential of *Selaginella doederleinii* to inhibit the proliferation and migration of the HTB-183 cell line of lung cancer.

**Keywords:** Selaginella doederleinii*, HTB-183, cytotoxicity, cell migration, in silico analysis*.

## INTRODUCTION

Data from the World Health Organization (2022) states that lung cancer is the second highest prevalence cancer in the world, with 2.21 million cases. Lung cancer is the cancer with the most increased mortality, with 1.80 million deaths. According to the International Agency for Research on Cancer (2020), lung cancer has the third highest prevalence in Indonesia, with 34,783 cases.

Submitted: February 09, 2024
Revised: March 10, 2024
Accepted: March 21, 2024
Published online: August 13, 2024
*Corresponding author: rifki.febriansah@umy.ac.id

Chemotherapy is the most widely used method in cancer treatment (Ramos, *et al*., 2021). However, it has many side effects, specifically drug resistance and toxicity. The failure of chemotherapy in 90% of cases occurs in the invasion and metastasis phase of cancer due to the drug resistance of cancer cells (Bukowski, *et al*., 2020). The development of cancer therapy with natural ingredients needs to be considered as an effort to avoid the systemic toxicity of chemotherapy. In addition, the combination of natural ingredients in chemotherapy is expected to broaden the therapeutic window and reduce drug resistance (Lin, *et al*., 2020).

*Selaginella doederleinii* is a beneficial plant in the Selaginellaceae family (Li, *et al*., 2020). Phytochemicals screening of the *S.doederleinii* plant showed high levels of bioflavonoids such as hinokiflavone, heveaflavone, amentoflavone, delicaflavone, 7,4′,7′′,4′′′-Tetra-O-methyl-amentoflavone, and others (Wang, *et al*., 2022). Biflavonoids from Selaginella species are known for remarkable antineoplastic activities, such as preventing cancer growth, inhibiting the metastasis process, and triggering apoptosis and autophagy properties of the cancer cells (Ren, *et al*., 2023). According to Xu, *et al.* (2022), the Ethyl acetate extract of *S.doederleinii* exhibited cytotoxic activity after 24 h of incubation towards A549 and PC9 lung cancer cell lines with $IC_{50}$ 92.88 µg/mL and 91.24 µg/mL, respectively.

HTB-183 is a brand name from the NCI-H661 cell line, which included large cell carcinoma types in the epithelial tissue of the human lung. According to the American Cancer Society (2018), large cell carcinoma is a sub-type of Non-Small Cell Lung Carcinoma (NSCLC). This type of cancer can develop in any part of the lung with a rapid progression that leads to difficulties in treatment.

This study aims to determine the anticancer activity of ethyl acetate extract of *Selaginella doederleinii* (EAESD) against HTB-183 lung cancer cells through *in silico* and *in vitro* approaches. This study is expected to be a reference source for further research and development of herbal plants in alternative and complementary medicine for anticancer therapy.

## MATERIALS AND METHODS

### Extraction

The *S. doederleinii* plants obtained were washed, dried, and then blended to form a powder. A total of 500 grams of powder dissolved using ethyl acetate solvent in a ratio of 1:10 was put into the macerator. The powder was soaked for five days and stirred to maximise the maceration process. Afterwards, re-maceration was done for two days. The result of the macerate was filtered, and the procedure was repeated three times with the same solvent. The macerate was concentrated with a rotary evaporator set at 100 rpm and a temperature of 50ºC followed by heating with a water bath at the same temperature to obtain dried ethyl acetate extract of *S. doederleinii* plant (Li, *et al*., 2020).

### HPLC Analysis

HPLC analysis was conducted by following the method from Li, *et al.* (2020), in which an amount of 20 mg of extract was dissolved in 1 ml of ethyl acetate, then filtered through a 0.45 µm membrane, and as much as 10 µL was injected into the HPLC. HPLC analysis was carried out with a UV detector system at 288 nm. The stationary phase used was the C18 column. The mobile phase was aqueous acetic acid (0.5% v/v) / eluent A and acetonitrile/eluent B. The elution gradient was as follows: 10% - 45% in 0-25 min, 45% -58% in 25-45 min, 58%-95% eluent B in 45-46 min, and 100% in 45-51 min. Re-equilibration was performed for 10 minutes, with a total running time of 51 minutes.

### *In Vitro* Analysis

#### Cytotoxic Assay

Cell preparation was done by thawing inactive HTB-183 cells at 37ºC. Cells were then centrifuged at 2500 rpm for 5 minutes; the

supernatant was discarded and then re-suspended with the addition of 1 mL of media. The medium used for culturing HTB-183 cells is Dulbecco's Modified Eagle's Medium (DMEM), which is added with 10% Fetal Bovine Serum, 2% penicillin-streptomycin, 0.5% amphotericin. The cells were incubated at 37ºC with 5% $CO_2$ flow until the appropriate number of cells was obtained or confluent (Chen, 2022). Cells are then harvested and transferred into fresh media for sub-culturing. The sub-culture procedure was done by spreading the cells in 96-well plates at a concentration of 10,000 cells/100 µL media for each well and incubating (Adam, *et al*., 2021).

After incubation, cells were treated with EAESD at 500, 250, 125, 65, and 32.5 ppm concentrations and incubated for 24 h. After treatment, MTT solution as a reagent was added to each well as much as 10 µl with a concentration of 0.5 mg/mL (Adam, *et al*., 2021). Incubation was carried out at 37°C for 4 h. After 4 h, the media with MTT was discarded and washed, and then 10% SDS stopper solution was added so that the formazan crystals dissolved. The plate was observed on an ELISA reader with a wavelength of 595 nm (Kristiani, *et al*., 2021). The viability of the cells is then calculated with the formula below:

**% Cell viability=(cell with treatment absorbance -medium control absorbance)/ (cell control absorbance-medium control absorbance) x100%**

### Migration Cell Assay

The extracellular matrix is made by culturing a certain number of cells, which in this study was $7.5x10^4$ cells. According to Martinotti (2020), 60-mm wide or multiwell plates such as 6-, 12-, and 24-well plates are used. In this study, cells were grown in 24-well plates. Incubation was carried out for 24 h at 37°C and circulated with 5% $CO_2$ (Pijuan, *et al*., 2019). Furthermore, scratches were made on the cell layer using a 200 µl-pipette tip (Han, *et al*., 2023). Cells were then treated at concentrations of $IC_{50}$, ½ $IC_{50}$, and ¼ $IC_{50}$. Migration speed was calculated using the formula according to Arnedo, *et al*. (2020):

**Migration Rate (RM) =(Scratch width at initial time (Wi)-Scratch widht at observation time (Wf))/(Duration of observation (t))**

### *In Silico* Analysis

### Bioinformatics Analysis

Prediction of Activity Spectra for Substances (PASS) analysis was conducted on the website http://www.way2drug.com/PASSOnline/. The possible pharmacological activity of each compound was obtained in the form of Probable Activity (Pa) and Probable Inactivity (Pi) with a range of values between 0.000 and 1.000 (Chowdhury & Bhattacharjee, 2021). The compound selection was conducted with PASS to determine the compounds with the most potential among 11 biflavonoids obtained in HPLC analysis.

The Protein-Protein Interaction (PPI) Network was established for three compounds with the highest Pa value. The proteins with correlation to the phytochemicals in EAESD were obtained through the Swiss Target Prediction Method through the website http://www.swisstargetprediction.ch/, and "homo sapiens" was chosen as the species (Sivasakthi, *et al*., 2021). Proteins obtained were collected in one file. Following that, genes regulating lung cancer were selected from PubMed with the keyword "Non-Small Cell Lung Cancer." The examination continued by creating a Venn diagram between proteins correlating to each compound and proteins regulating NSCLC using the website http://www.interactivenn.net. Proteins that intersect on the diagram were arranged into the PPI networks through https://string-db.org, and the degree scores were obtained through Cytoscape version 3.8.2.

### Molecular Docking

The proteins with the highest degree score from PPI networks established in the previous method were used as molecular docking targets. The protein structures were searched on the site www.rcsb.org and downloaded in .pdb format. The proteins and ligand natives were prepared through the DS visualizer and Autodock Tools. Autodock Tools is also used to set the Gridbox from the native ligand and protein linkage process, resulting in x,y, and z values, which are recorded for the docking process using Autodock Vina (Susanti, *et al*., 2018). Determination of the RMSD value was done by filling in the Windows Command Prompt or CMD according to the code so that several conformations would appear. Each conformation shows the value of RMSD. In this study, the conformations with RMSD value less than 2 Å were chosen for visualisation, which was done by using the Discovery Studio Visualizer application (Susanti, *et al*., 2018).

## RESULTS

### Extraction

From the extraction process, dark green ethyl acetate extract of *S. doederleinii* (EAESD) was obtained as much as 17.401 grams, or a rendemen of 3.48%, from 500 grams of dried powder before extraction.

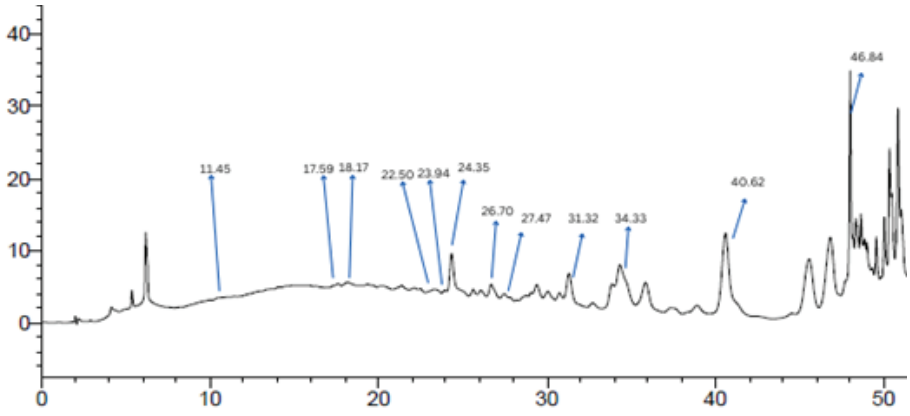


**Figure 1. EAESD chromatogram.**

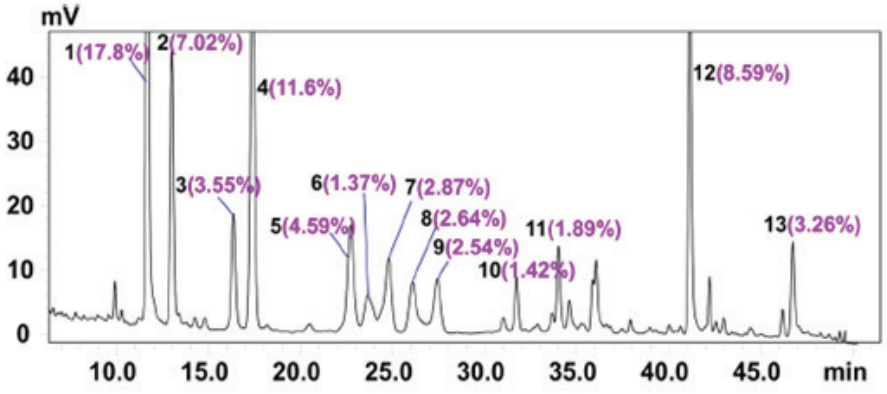


**Figure 2. Chromatogram of *S. Doederleinii* according to Li, *et al*. (2020).**

Indonesian Journal of Cancer Chemoprevention, February 2024
ISSN: 2088–0197
e-ISSN: 2355-8989

## High Performance Liquid Chromatography (HPLC)

The EAESD chromatogram results were obtained to be qualitatively analysed with the comparison of Rt compounds in the previous study by Li, *et al*. (2020), which was also a reference for the chromatographic system.

The EAESD compound content was analysed using the same HPLC system as the previous study by Li, *et al*. (2020). The chromatogram results obtained were then compared with chromatograms from the same literature. In this study, 12 peaks were obtained with retention times similar tothose in previous research, as seen in Table 1.

**Table 1. Retention time comparison of EAESD to the previous literature.**

| Compounds | Retention Time of Literature (Li, et *al*., 2020) (Minutes) | Retention Time of EAESD (Minutes) |
|---|---|---|
| Amentoflavone | 11-12 | 11.45 |
| Robustaflavone | 13 | - |
| 2,3-Dihydro-3,3-biapigenin | 16-17 | 17.59 |
| 3,3-Binaringenin | 18-19 | 18.17 |
| Delicaflavone | 22-23 | 22.50 |
| Unknown | 23-24 | 23.94 |
| Hinokiflavone | 24-25 | 24.35 |
| 2,3- Dihydrohinokiflavone | 26-27 | 26.70 |
| Chrysocauloflavone | 27-28 | 27.47 |
| 2,3- Dihydroisocryptomerin | 31-32 | 31.32 |
| Robustaflavone 7,4-dimethyl ether | 34 | 34.33 |
| Heveaflavone | 40-41 | 40.62 |
| 7,4',7'',4'''-Tetra-O-methyl-amentoflavone | 47 | 46.844 |

## *In Vitro* Analysis

### Cytotoxic Assay

In MTT analysis, absorbance values from the ELISA reader on EAESD samples and Carboplatin control were used to calculate cell proliferation. The proliferation or viability values were then analysed using linear regression for their correlation with different sample concentrations. From the linear regression equation obtained, the $IC_{50}$ value can be determined. In this study, the linear regression equation of EAESD was y=-0.1609x+80.58 and the $IC_{50}$ value of 190 µg/mL was obtained. Meanwhile, the linear regression equation of Carboplatin control is y=-0.1303x+109.46, with an $IC_{50}$ value of 456 µg/mL.

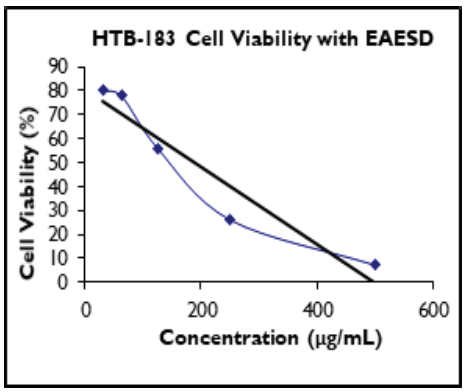


**Figure 3. Linear regression of cell viability with different EAESD concentration.**

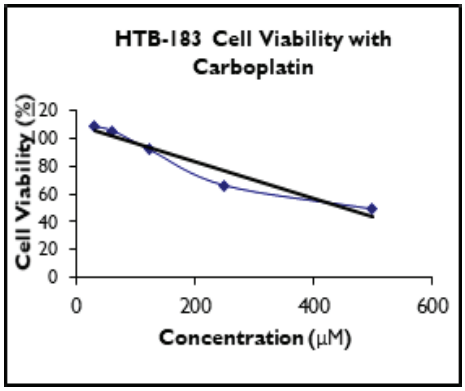


**Figure 4. Linear regression of cell viability with different carboplatin concentration.**

## Migration Cell Assay

Table 2. Result of migration rate and changes in scratch width during the observation.

| Treatment | Migration Rate (Rm) (µm/hour) | | | Average of Total Rm (µm/hr) |
|---|---|---|---|---|
| | 3rd Hour | 6th Hour | 18th Hour | |
| Cell Control | 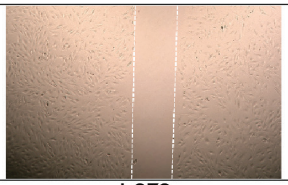 1.879 | 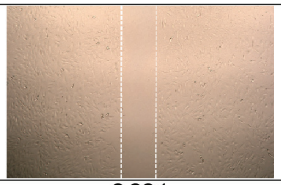 2.224 | 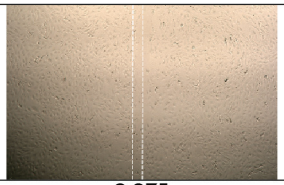 2.875 | 2.326 |
| $IC_{50}$ Conc. EAESD (190 µg/ml) | 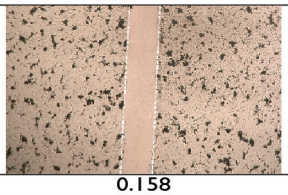 0.158 | 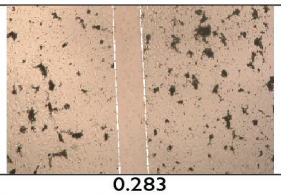 0.283 | 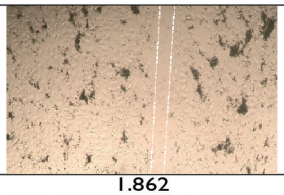 1.862 | 0.768 |
| ½ $IC_{50}$ Conc. EAESD (95 µg/ml) | 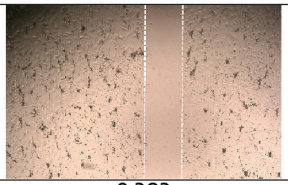 0.383 | 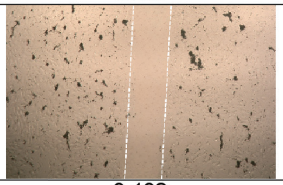 0.409 | 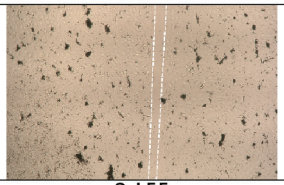 2.155 | 0.982 |
| ¼ $IC_{50}$ Conc. EAESD (47 µg/ml) | 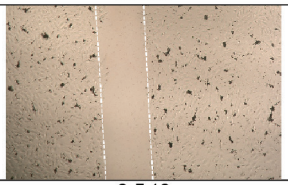 0.540 | 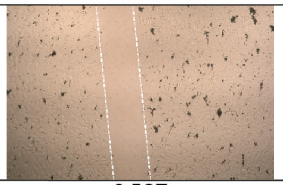 0.597 | 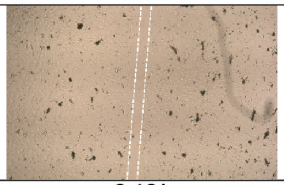 2.681 | 1.273 |
| $IC_{50}$ Conc. Carboplatin (456 µg/ml) | 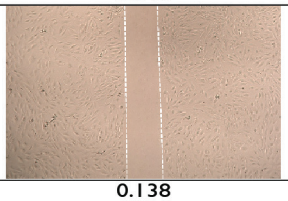 0.138 | 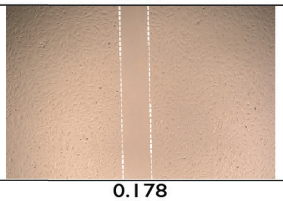 0.178 | 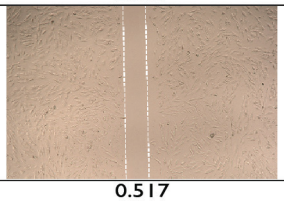 0.517 | 0.278 |
| ½ $IC_{50}$ Conc. Carboplatin (228 µg/ml) | 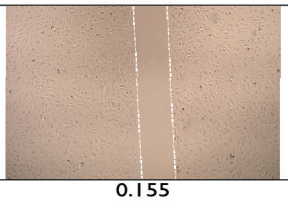 0.155 | 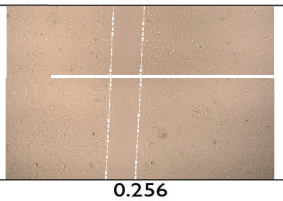 0.256 | 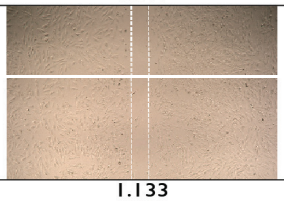 1.133 | 0.515 |
| ¼ $IC_{50}$ Conc. Carboplatin (114 µg/ml) | 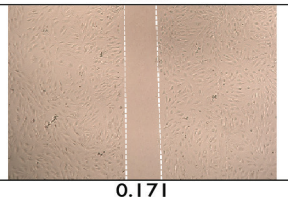 0.171 | 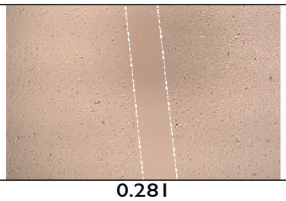 0.281 | 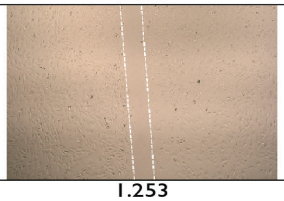 1.253 | 0.568 |

The result of the migration assay can be shown in the picture; the gap of the cell layer can be observed and measured occasionally. The EAESD sample showed some black dots at the cell layer, considering the fractions of EAESD that were undissolved in the growth medium due to different polarities. DMEM is a soluble water compound. Meanwhile, EAESD consists of compounds with different polarity ranges. However, the undissolved fractions are attached to the cell layer and follow the cell movement; thus, the scratched gap changes can be easily observed and measured. The gap changes are measured to determine the cell migration rate. The average migration rate at all observation times in the control cells was 2.326 µm/h. In the treatment with EAESD, with the doses of $IC_{50}$ 190 µg/ml, ½ $IC_{50}$ 95 µg/ml, and ¼ $IC_{50}$ 47 µg/ml, the average migration rates were 0.768 µg/ml, 0.982 µg/ml, and 1.273 µg/ml respectively. In the treatment with Carboplatin doses of $IC_{50}$ 456 µg/ml, ½ $IC_{50}$ 228 µg/ml, and ¼ $IC_{50}$ 114 µg/ml, the average migration rates for the entire observation time were 0.278 µm/h, 0.515 µm/h, and 0.568 µm/h. The smaller the migration rate, the greater the ability to inhibit cell migration from the treatment.

## *In Silico* Analysis Bioinformatics

In PASS analysis, five compounds with probable activity as anti-lung cancer were obtained, namely robustaflavone 7,4-dimethyl ether, 7,4',7'',4'''-tetra-O-methyl-amentoflavone, heveaflavone, amentoflavone, and hinokiflavone.

Table 3. Result of PASS of five compounds with anti-lung cancer activity.

| Compounds | Anti-Lung Cancer Activity | |
|---|---|---|
| | Probable Activity (Pa) | Probable Inactivity (Pi) |
| Robustaflavon 7,4-dimethyl eter (R7D4ME) | 0.427 | 0.020 |
| Heveaflavone | 0.416 | 0.021 |
| 7,4',7'',4'''-tetra-O-methyl-amentoflavone (7474TOMA) | 0.416 | 0.021 |
| Amentoflavon | 0.390 | 0.024 |
| Hinokiflavone | 0.377 | 0.027 |

The three compounds with the highest probable activity, such as Robustaflavon 7,4-di-methyl ether (R7D4ME), Heveaflavone, and 7,4',7'',4'''-tetra-O-methyl-amentoflavone (7474TOMA) were selected to be analysed to obtain a PPI network. The PPI network obtained for each compound is shown in the tables below:

Table 4. Protein targets and PPI network of R7D4ME.

| Proteins | Degree Score | Visualisation |
|---|---|---|
| EGFR | 46 | 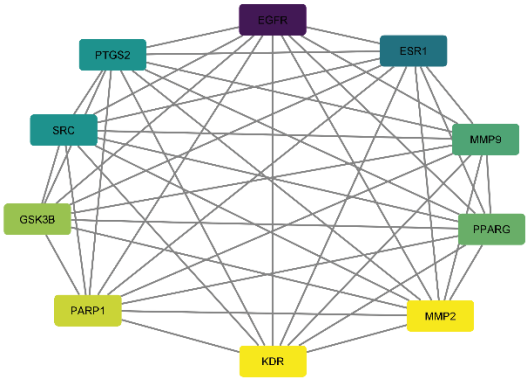 |
| ESR1 | 37 | |
| PTGS23 | 7 | |
| SRC3 | 5 | |
| MMP9 | 34 | |
| PPARG3 | 2 | |
| GSK3B3 | 0 | |
| PARP12 | 8 | |
| MMP2 | 28 | |
| KDR1 | 9 | |

Table 5. Protein targets and PPI network of heveaflavone.

| Proteins | Degree Score | Visualisation |
|---|---|---|
| ESR1 | 33 | 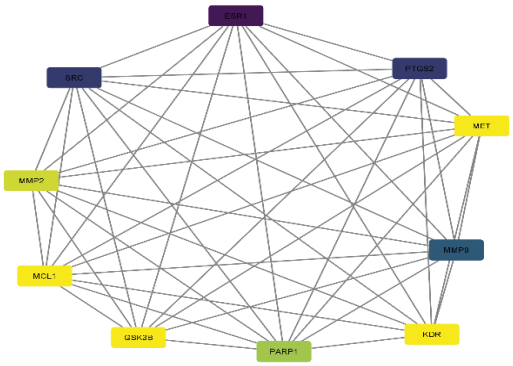 |
| PTGS23 | 1 | |
| SRC3 | 1 | |
| MMP93 | 0 | |
| PARP12 | 5 | |
| MMP22 | 4 | |
| KDR2 | 3 | |
| MET2 | 3 | |
| GSK3B2 | 3 | |
| MCL1 | 23 | |



Table 6. Protein targets and PPI network of 7474TOMA.

| Protein | Degree Score | Visualisation |
|---|---|---|
| TNF3 | 9 | 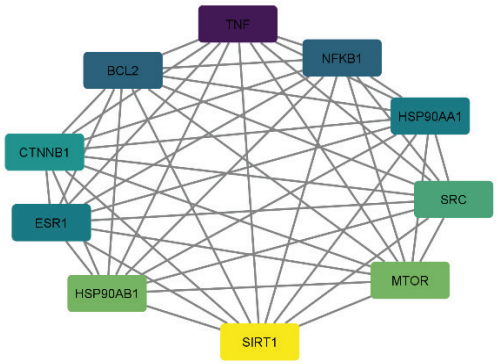 |
| NFKB13 | 5 | |
| BCL2 | 35 | |
| HSP90AA1 | 34 | |
| ESR1 | 34 | |
| CTNNB1 | 33 | |
| SRC3 | 2 | |
| MTOR | 31 | |
| HSP90AB1 | 31 | |
| SIRT12 | 8 | |



Proteins with the highest degree score from each PPI network of the compounds were prepared for further analysis in Molecular Docking.

## Molecular Docking

The visualisation, docking score, and RMSD value of each compound and its control towards the Hubb proteins are listed in the table below:

Table 7. Result of molecular docking.

| Proteins | Compounds | RMSD | Docking Score | Conformation |
|---|---|---|---|---|
| EGFR | R74DME | 1.174 | -9.2 | 9 |
| | Mobocertinib (Control) | 1.845 | -7.2 | 7 |
| ESR1 | Heveaflavone | 1.830 | -9.5 | 2 |
| | Elacestrant (Control) | 1.307 | -5.9 | 6 |
| TNF | 7474TOMA | 1.668 | -6.5 | 8 |
| | Thalidomide (Control) | 0.808 | -6.5 | 2 |

Indonesian Journal of Cancer Chemoprevention, February 2024
ISSN: 2088–0197
e-ISSN: 2355-8989

Table 5. Result visualization of molecular docking.

| Proteins | Compounds | 2D Visualization | 3D Visualization |
|---|---|---|---|
| EGFR | R74DME | 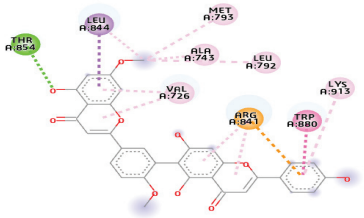 | 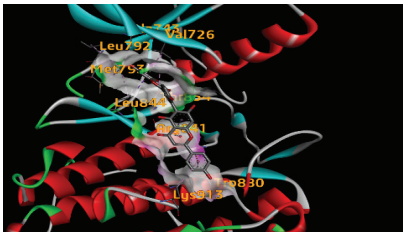 |
| | Mobocertinib | 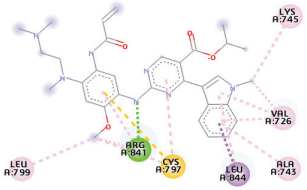 | 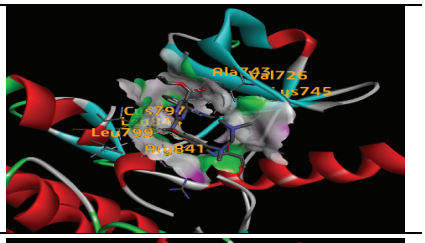 |
| ESR1 | Heveaflavone | 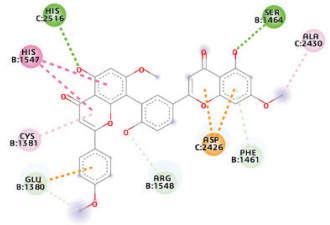 | 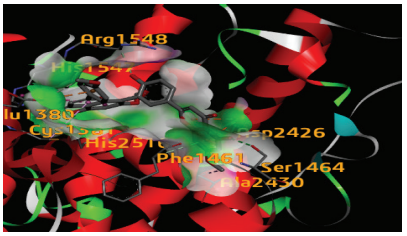 |
| | Elacestrant | 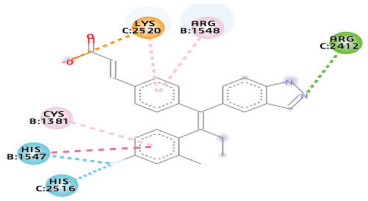 | 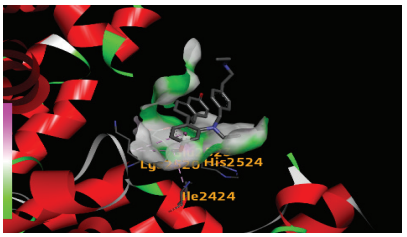 |
| TNF | 7474TOMA | 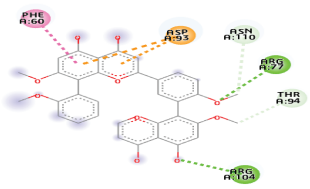 | 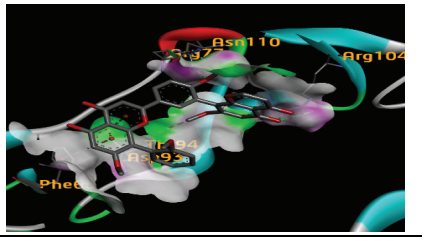 |
| | Thalidomide | 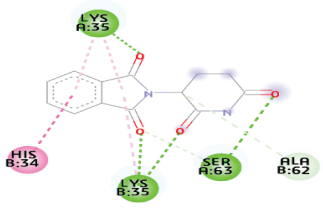 | 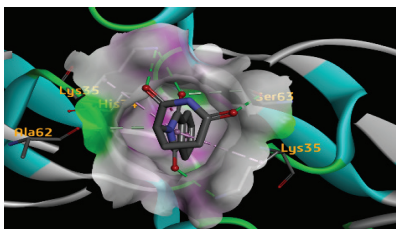 |

The result of the molecular docking visualization showed the chemical interactions between the compounds and the amino acids from the targeted protein. The dark green color in the 2D visualization result indicated conventional hydrogen bonds, the light green indicated pi-donor hydrogen bonds or carbon-hydrogen bonds, the orange color indicated pi-anion or pi-cation interaction, the purple color indicated pi-sigma bonds, the dark pink indicated pi-pit-shaped bonds, and the pink color indicated alkyl or pi-alkyl bonds. The amino acid where the interaction predicted to occur written in abbreviation of three letters which can be observed in the pictures.

## DISCUSSION

*Selaginella doerderleinii* is known for its high content of bioflavonoids, which have shown anticancer and antitumor effects on various cancer cells in previous studies (Li, *et al*., 2017; Kang, *et al*., 2021; Muemba, *et al*., 2022). High Performace Liquid Chromatography was used in this research to evaluate the biflavonoids content of EAESD. The gradient mobile phase optimised the separation and decreased the analysis duration among the compounds with various polarity contained in EAESD Rehman & Qamar (2022). The chromatography system followed Li, *et al*. previous study (2020), and the chromatogram obtained was then compared to the same literature. Twelve peaks with a retention time similar to the biflavonoids shown in the literature were obtained. Thus, it can be assumed that EAESD consists of compounds such as Amentoflavone, Robustaflavone, 2,3-Dihydro-3,3-biaπgenin, 3,3-Binaringenin; Delicaflavone, Hinokiflavone; 2,3- Dihydrohinokiflavone, Chrysocauloflavone, 2,3- Dihydroisocryptomerin, Robustaflavone 7,4-dimethyl ether; Heveaflavone; 7,4',7'',4'''-Tetra-O-methyl-amentoflavone, and one unidentified compound. The phytochemical contents of EAESD observed in the HPLC result showed slight differences in retention times and peaks of compounds compared to the result of the literature reference. The different habitats of *S. doederleinii* samples are considered to be the reason. The variation of phytochemicals from a plant species can be affected by environmental factors such as soil conditions, altitude, pH, light, *etc* (Bazargani, *et al*., 2020). Thus, the phytochemicals of the *S. doederleinii* plant can vary from one area to another.

Cytotoxicity activity of EAESD towards HTB-183 cell observed through MTT Assay. In this case, the $IC_{50}$ value is used as a cytotoxicity parameter, where this value is defined as the concentration of the drug or sample that inhibits cell growth among 50% of the cultured population (Ali, *et al.*, 2021). This study obtained the $IC_{50}$ value of 190.055 µg/mL. In other words, at a 190.055 µg/mL concentration, the EAESD can kill 50% of the HTB-183 cell population. Meanwhile, the $IC_{50}$ value of Carboplatin as the control was 456.331 µg/mL, showing that at that concentration, Carboplatin can trigger the death of 50% of the HTB-183 cell population. In this study, the cytotoxic activity of EAESD against HTB-183 cells is significantly more potent than carboplatin based on the smaller $IC_{50}$ value. Consequently, it is suggested that EAESD has the potential to be developed as a lung anticancer agent.

The ability of the EAESD to inhibit cell migration was further assessed using the wound scratch healing assay method. The observation of cell migration at the 3$^{rd}$, 6$^{th}$, and 18$^{th}$ h showed that the concentration of the sample influenced the inhibition of cell migration. In the treatment with EAESD and Carboplatin, the ability to inhibit cell migration decreased as the concentration decreased. The slower the migration rate, the greater the ability of a compound to inhibit cell migration. The cell migration rate in both EAESD and Carboplatin treatment is still lower compared to the control cells, as shown from the first observation at the 3$^{rd}$ h.

The average migration rate calculation showed that Carboplatin can inhibit cell migration better than EAESD. Nevertheless, EAESD still can inhibit cell migration compared to the control, although at a minor concentration of ¼ of the $IC_{50}$ value. Therefore, EAESD is considered to have still the potential to inhibit migration in HTB-183 lung cancer cells.

The highest sample concentration is based on the $IC_{50}$ value from the MTT Assay cytotoxic analysis, which represents the cell proliferation value. High cell proliferation will increase the density of cultured cells so that cells will tend to move and migrate towards areas with lower density (Gallaher, *et al*., 2018). At concentrations of ½ and ¼ $IC_{50}$, the ability of EAESD and Carboplatin to inhibit cell proliferation tends to decrease, so the rate of cell migration also drops. Cell migration patterns influenced by density also correlate with quorum sensing mechanisms. Quorum sensing is an intercellular communication mechanism that coordinates gene expression, which then affects the collective behaviour of cells based on their population density. This mechanism is caused by the ability of cells to perceive their population density along with other cells in an environment. Responses to changes in cell density are then coordinated through changes in gene expression and signalling proteins (Antonioli, *et al.*, 2019). The mechanism of cell migration inhibition and cytotoxicity of EAESD and the proteins involved were predicted using *in silico* methods.

Previous *in silico* studies to analyse the activities of heveaflavone, R74DME, and 7474 TOMA had been conducted. A study by Kumar, *et al* (2023), showed the ability of heveaflavone to bind with several proteins regulating NSCLC, such as AKT1, VEGFA, and GSK3B. Another study by Mohammed, *et al* (2022), showed the interaction of R74DME to HSP90A, EGFR, and P53 proteins. However, these studies did not compare the binding affinity value between heveaflavone and control compounds, which had been scientifically proven to inhibit the protein targets. Meanwhile, there is limited data regarding the ability of 7474TOMA to bind with disease-regulating proteins. A study by Rajaei, *et al* (2023), did not show the the ability of 7474TOMA to bind to P-gp protein. This study evaluated the affinity of the compounds towards proteins that regulate NSCLC involving control compounds as the comparison. The bioinformatics as the initial study was conducted through PASS, Swiss Target Prediction, and STRING to obtain PPI networks. Hence, the hub proteins or proteins with the highest score in each PPI network can be determined as the molecular docking targets for each compound.

The *in silico* method began with the PASS (Prediction of Activity Spectra for Substances) method. Of the 11 compounds that detected in EAESD according to HPLC analysis, five compounds with lung anticancer activity were amentoflavone (Pa: 0.390 and Pi: 0.024), hinokiflavone (Pa: 0.377, Pi: 0.027), heveaflavone (Pa: 0.416, Pi: 0.021) robustaflavone 7,4-dimethyl ether (Pa: 0.390, Pi: 0.020), and 7,4’,7’,4’’-tetra-O-methyl-amentoflavone (Pa: 0.416, Pi: 0.021).). Pa stands for probable activity, and Pi stands for Probable inactivity. All the compounds obtained probable activity less than 0.5; in that case, the probability of discovering new chemical compounds is high, yet the likelihood of getting pharmacological activities through *in vitro* assays is presumed low (Fakih, *et al*., 2021). Three compounds with the highest probable activity value, such as heveaflavone, R74DME, and 7474TOMA, were prepared for further *in silico* analysis.

Protein-protein interaction networks were established among the proteins that regulate NSLC and can bind to the analysed compound. In this step, the degree score is also observed. The degree score of a protein is a number that describes the number of interactions associated with the protein. Proteins with high degree score values are called hub proteins with the most significant connections and are assumed to play a crucial role in the network

between proteins in the PPI Network (Prava & Pan, 2022). Hub proteins from each PPI network of the compounds were prepared for molecular docking. Those proteins are EGFR for R74DME, ESR1 for Heveaflavone, and TNF for 7474TOMA.

The obtained proteins are crucial in the progression of lung cancer. EGFR, or Epidermal Growth Factor, is a tyrosine kinase inhibitor made of an extracellular domain, a transmembrane domain, and an intercellular domain connected to activator and receiver kinase domains with C-terminal and phosphorylated tyrosin tails (Tamirat, *et al*., 2019). The mutation in EGFR will affect the correlated signalling pathways such as RAS, KAK, PI3-K, MEK, mTOR, and STAT, further interrupting gene transcription that regulates the proliferation and migration process (Hsu, *et al*., 2019). The mutation in this receptor mainly occurred in NSCLC patients with adenocarcinoma type and patients with Asian ethnicity (O'Leary, *et al*., 2020). The other analysed protein is ESR1 or Estrogen Receptors Alfa, a nuclear hormone receptor known to regulate breast cancer (Grinshpun, *et al*., 2023). According to a bioinformatics study by Gao, *et al*. (2019), this receptor significantly impacted NSCLC progression by affecting several NSCLC-related pathways, such as Wnt/β-Catenin, EGFR, and Notch. This study also analysed TNF, or Tumor Necrosis Factor, as a protein target. TNF is included in cytokine groups and ruled in many biological conditions, such as cell proliferation, inflammation, and immune reactions. Inhibition of TNF receptors will affect other cellular pathways related to lung cancer prognosis, such as EGFR and NF-KB, which alter the transcription of survival genes (Gong, *et al*., 2021).

Compounds and drugs approved according to previous studies to target the mentioned proteins, such as Mobocertinib, Elacestrant, and Thalidomide, were used as the controls. Mobocertinib is a novel compound that exhibited inhibitory activity towards 14 of 15 EGFR models that have been analysed (Gonzalves, *et al*., 2021). This study used Mobocertinib as the control compound of R74DME in Molecular Docking. Thus, the binding affinity of each compound towards EGFR can be compared. Meanwhile, Elacestrant, an FDA-approved drug that can inhibit ESR1 (Varella & Cristofanilli, 2023), was used as the control compound for Heveaflavone. Another control compound is Thalidomide, famous for its teratogenicity effect but re-approved as an antiflamation agent with a significant ability to bind to TNF-α (Shivaleela, *et al*., 2021).

Molecular docking is performed to examine the conformation and orientation (also known as the pose) of the ligand molecules towards the binding site of a targetted protein (Torres, *et al*., 2019). From the scoring function, the RMSD or Root Mean Square Deviation value is obtained to compare the accuracy of each docking conformation. A good RMSD value describes the condition where the atoms of the ligands match each other, and the symmetric atoms are considered equivalent. An acceptable RMSD value ranges from 2.0 to 3.0 Å (Ramirez and Caballero, 2018). From the overall docking results of each compound against its hub protein, conformations were obtained in the range of values below 2 Å so that these conformations can be used to determine the docking score and visualisation of docking results.

The interaction between the compound and the protein can affect the docking score. The bond between a ligand and a receptor governs the energy of the bond formed, especially non-covalent interactions, which consist of hydrogen bondings, hydrophobic, π-π, ionic, and van der Waals interactions (Zhuang, *et al*., 2019). In some studies, the number of hydrogen bonds positively correlates to the interaction stability among the compounds and the protein target (Arthur, (2019); Arthur and Uzairu (2019); Lagares, *et al*., (2020)). Hydrophobic and electrostatic interac-

tions also showed a stronger bond between ligands and the receptor (Chaubah, *et al*., 2019). Another crucial interaction is phi bonding interactions (Pi-alkyl, pi-stacked, and pi-sigma), which appear to support a compound's high affinity towards the target (Arthur & Uzairu,2019; Shen, 2021). The 3D and 2D visualisation showed that all analysed compounds exhibited hydrogen, hydrophobic, electrostatic, and phi bonding interactions towards the proteins, which altered their binding affinity.

The docking score or binding affinity is the binding energy value of a ligand to a receptor and is expressed in units of kcal/mol. This binding energy value is the total intermolecular interactions between the ligand and the receptor after being linked, which can also be expressed in Gibs free energy bond (ΔGL). Docking conformation with the lowest value represents the best result (Ortegon, *et al*., 2022). In this study, the docking score of R74DME was -9.2 kcal/mol, lower than the control Mobocertinib with -7.2 kcal/mol affinity towards the EGFR protein. A similar result was obtained in the docking process of Heveaflavone towards ESR1, which was -9.5 kcal/mol and significantly higher than the control Elacestrant -5.9 kcal/mol. Meanwhile, 7474TOMA showed the same score as Thalidomide as the control toward TNF. According to this result, it can be presumed that all of the analysed compounds have the potential to bind to each protein target that regulates NSCLC.

## CONCLUSION

According to the research which has been done, EAESD contains bioflavonoids according to HPLC analysis. *In vitro* analysis towards EAESD showed cytotoxic activity towards lung cancer HTB-183 cells with $IC_{50}$ 190.055 µg/mL. Cell migration inhibitory properties were also observed at concentrations of $IC_{50}$ (190.055 µg/mL), ½ $IC_{50}$ (95.05 µg/mL), and ¼ $IC_{50}$ (47.51 µg/mL). The data obtained from *in silico* analysis using Bioinformatics suggested three compounds with the highest probable activity as anti-lung cancer compounds according to PASS such as robustaflavone 7,4-dimethyl ether (R74DME) Pa 0.427: Pi 0.20, Heveaflavone Pa 0.416: Pi 0.021, and 7,4',7'',4'''-tetra-O-methyl-amentoflavone (7474TOMA) Pa 0.416: Pi 0.021. The hub proteins for each compound were also obtained, such as EGFR, ESR1, and TNF, respectively. Interactions of the compounds towards each hub protein were evaluated using molecular docking methods involving inhibitors of the proteins as the controls. Mobocertinib was used as the control compound of EGFR, Elacestrant as the control compound of ESR1, and Thalidomide as the control compound of TNF. The docking score obtained for EGFR was -9.2 kcal/mol with R7D4ME and -7.2 kcal/mol with the control Mobocertinib. The docking score of ESR1 was -9.5 kcal/mol with heveaflavone and -5.9 kcal/mol with the control Elacestrant. As for TNF, the score was -6.5 for both 7474TOMA and Thalidomide as the control compound. This study suggested a remarkable potential of EAESD as a proliferation and migration inhibitor agent towards HTB-183 lung cancer cells according to *in silico* and *in vitro* approaches. Further advanced *in silico* and *in vitro* research regarding this topic is needed to evaluate the toxicity of EAESD towards normal cells and the specific pharmacological mechanism of the anticancer properties.

## ACKNOWLEDGMENTS

The authors thank the School of Pharmacy of Universitas Muhammadiyah Yogyakarta and ObatApps Platform for supporting this research. The authors would also like to thank Dr. Hong Yao from Fujian Medical University for his suggestion regarding the detailed steps of *S. doederleinii* sample preparation for HPLC

analysis; Mr. Fajar Aji Lumakso from Universitas Ahmad Dahlan for his help and guidance regarding the HPLC procedures; and Mr. Adi Hermawansyah from the Cell Culture Laboratory of Universitas Muhammadiyah Yogyakarta for his help and guidance regarding the *in vitro* (MTT Assay and Wound Scratch Healing Assay) procedures.

## REFERENCES

Adam, S.H., Darrag, A., and Abdelsalam, N., 2021, Comparative evaluation of the cytotoxic effect of different intracanal medicaments, *Dental Science Updates*, **2**(2), 123-133.

Ali, A., Banerjee, S., Kamaal, S., Usman, M., Das, N., Afzal, M., *et al*., 2021, Ligand substituent effect on the cytotoxicity activity of two new copper (ii) complexes bearing 8-hydroxyquinoline derivatives: Validated by MTT assay and apoptosis in MCF-7 cancer cell line (human breast cancer), *RSC advances*, **11**(24), 14362-14373.

American Cancer Society, 2018, Cancer Facts and Figures 2018. Accessed at 7 June 2022, from Cancer: https://www.cancer.org/content/dam/cancer-org/research/cancer-facts-and-statistics/annual-cancer-facts-and-figures/2018/cancer-facts-and-figures-2018.pdf

Antonioli, L., Blandizzi, C., Pacher, P., Guilliams, M., and Haskó, G., 2019, Rethinking communication in the immune system: the quorum sensing concept, *Trends in immunology*, **40**(2), 88-97.

Arthur, D.E., 2019, Molecular docking studies of some topoisomerase II inhibitors: Implications in designing of novel anticancer drugs, *Radiology of Infectious Diseases*, **6**(2), 68-79.

Arthur, D.E., and Uzairu, A., 2019, Molecular docking studies on the interaction of NCI anticancer analogues with human Phosphatidylinositol 4, 5-bisphosphate 3-kinase catalytic subunit, *Journal of King Saud University-Science*, **31**(4), 1151-1166.

Bukowski, K., Kciuk, M., and Kontek, R., 2020, Mechanisms of Multidrug Resistance in Cancer Chemotherapy, *International Journal of Molecular Science*, **21**(3233), 1-24.

Chaubah, M.A.L., Bontes, B.W., and Mulachelah, N.A., 2019, Molecular docking of polycyclic aromatic hydrocarbons as potentially carcinogenic molecules through binding with aryl hydrocarbon receptor, *Journal of Smart Bioprospecting and Technology P-ISSN*, 2686, 0805.

Chen, W., Cheng, H., and Xia, W., 2022, Construction of Polygonatum sibiricum Polysaccharide Functionalized Selenium Nanoparticles for the Enhancement of Stability and Antioxidant Activity, *Antioxidants*, **11**(2), 240.

Chowdhury, S.A., and Bhattacharjee, S.C., 2021, *In Silico* Biological Profile Prediction of Some Selectively Synthesized Acyl Rhamnopyranosides, *Journal of Scientific Research*, **13**(2), 657-668

Fakih, T.M., Ramadhan, D.S.F., and Darusman, F., 2021, *In silico* activity identification of cyclo peptide alkaloids from Zizyphus spina-christi species against Sars-Cov-2 main protease, *Jurnal Biodjati*, **6**(1), 71-81.

Filimonov, D.A., Lagunin, A.A., Gloriozova, T.A., Rudik, A.V., Druzhilovskii, D.S., Pogodin, P.V., and Poroikov, V.V., 2014, Prediction of The Biological Activity Spectra of Organic Compounds Using The Pass Online Web Resource, *Chemistry of Heterocyclic Compounds*, pp. 444–457.

Gallaher, J.A., Brown, J.S., and Anderson, A.R., 2019, The impact of proliferation-migration tradeoffs on phenotypic evolution in cancer, *Scientific reports*, **9**(1), 1-10.

Gao, X., Cai, Y., Wang, Z., He, W., Cao, S., Xu, R., and Chen, H., 2019, Estrogen receptors promote NSCLC progression by modulating the membrane receptor signaling network: a systems biology

perspective, *Journal of Translational Medicine*, **17**, 1-15.

García-Ortegón, M., Simm, G.N., Tripp, A.J., Hernández-Lobato, J.M., Bender, A., and Bacallado, S., 2022, DOCKSTRING: easy molecular docking yields better benchmarks for ligand design, *Journal of chemical information and modelin*g, **62**(15), 3486-3502.

Gong, K., Guo, G., Beckley, N., Zhang, Y., Yang, X., Sharma, M., and Habib, A.A., 2021, Tumor necrosis factor in lung cancer: Complex roles in biology and resistance to treatment, *Neoplasia*, **23**(2), 189-196.

Gonzalvez, F., Vincent, S., Baker, T.E., Gould, A. E., Li, S., Wardwell, S.D., *et al*., 2021, Mobocertinib (TAK-788): a targeted inhibitor of EGFR exon 20 insertion mutants in non–small cell lung cancer, *Cancer discovery*, **11**(7), 1672-1687.

Grinshpun, A., Chen, V., Sandusky, Z.M., Fanning, S.W., and Jeselsohn, R., 2023, ESR1 activating mutations: From structure to clinical application, *Biochimica et Biophysica Acta (BBA)-Reviews on Cancer*, **1878**(1), 188830.

Han, J., Xie, C., Liu, B., Wang, Y., Pang, R., Bi, W., *et al*., 2023, Tetraspanin 1 regulates papillary thyroid tumor growth and metastasis through c-Myc-mediated glycolysis, *Cancer Science*, **114**(12), 4535–4547.

Hsu, P.C., Jablons, D.M., Yang, C.T., and You, L., 2019, Epidermal growth factor receptor (EGFR) pathway, yes-associated protein (YAP) and the regulation of programmed death-ligand 1 (PD-L1) in non-small cell lung cancer (NSCLC), *International Journal of Molecular Sciences*, **20**(15), 3821.

International Agency for Research on Cancer, 2020, Cancer Incident in Indonesia. Diakses pada 6 Mei 2022, from Global Cancer Observatory: https://gco.iarc.fr/today/data/factsheets/populations/360-indonesia-fact-sheets.pdf

Jamkhande, P.G., Pathan, S.K., and Wadher, S.J., 2016, *In silico* PASS analysis and determination of antimycobacterial, antifungal, and antioxidant efficacies of maslinic acid in an extract rich in pentacyclic triterpenoids, *International Journal of Mycobacteriology*, **5**(4), 417-425.

Kang, F., Zhang, S., Chen, D., Tan, J., Kuang, M., Zhang, J., *et al*., 2021, Biflavonoids from *Selaginella doederleinii* as potential antitumor agents for intervention of non-small cell lung cancer, *Molecules*, **26**(17), 5401.

Kristiani, E.B.E., Kasmiyati, S., and Herawati, M., 2021, The cytotoxic and apoptotic effects of wild and polyploidy genotype of Artemisia cina extracts on the WiDr colon and HTB-183 lung cancer cell lines, *Biodiversitas Journal of Biological Diversity*, **22**(7), 2844-2852

Kumar, S., Abbas, F., Ali, I., Gupta, M.K., Kumar, S., Garg, M., and Kumar, D., 2023, Integrated network pharmacology and *in-silico* approaches to decipher the pharmacological mechanism of *Selaginella tamariscina* in the treatment of non-small cell lung cancer, *Phytomedicine plus*, **3**(2), 100419.

Li, D., Qian, Y., Tian, Y.J., Yuan, S. M., Wei, W., and Wang, G., 2017, Optimization of ionic liquid-assisted extraction of biflavonoids from *Selaginella doederleinii* and evaluation of its antioxidant and antitumor activity, *Molecules*, **22**(4), 586.

Li, S., Wang, X., Wang, G., Shi, P., Lin, S., Xu, D., *et al*., 2020, Ethyl acetate extract of *Selaginella doederleinii* hieron induces cell autophagic death and apoptosis in colorectal cancer via PI3K-Akt-mTOR and AMPKα-signaling pathways, *Frontiers in Pharmacology*, **11**, 565090.

Lin, S.-R., Chang, C.-H., Hsu, C.-F. H., Tsai, M.-J., Cheng, H., Leong, M. K., *et al*., 2020, Natural compounds as potential adjuvants to cancer therapy: Preclinical evidence, *British Journal of Pharmacology*, **177**, 1409-1423.

Martinotti, S., and Ranzato, E., 2019, Scratch wound healing assay, *Epidermal cells: methods and*

*protocols*, **2109**, 225-229.

Mohamed, M.E., Tawfeek, N., Elbaramawi, S.S., Elbatreek, M.H., and Fikry, E., 2022, Agathis robusta bark extract protects from renal ischemia-reperfusion injury: phytochemical, *in silico* and *in vivo* studies, *Pharmaceuticals*, **15**(10), 1270.

Mohammadi Bazargani, M., Falahati-Anbaran, M., and Rohloff, J., 2021, Comparative analyses of phytochemical variation within and between congeneric species of *Epilobium hirsutum* and *E. parviflorum*: contribution of environmental factors, *Front. Plant Sci.*, **11**, 595190.

Mohammadi, A., Mansoori, B., Duijf, P.H., Safarzadeh, E., Tebbi, L., Najafi, S., *et al.*, 2021, Restoration of miR-330 expression suppresses lung cancer cell viability, proliferation, and migration, *Journal of cellular physiology*, **236**(1), 273-283.

Mora Lagares, L., Minovski, N., Caballero Alfonso, A. Y., Benfenati, E., Wellens, S., Culot, M., *et al.*, 2020, Homology modeling of the human P-glycoprotein (ABCB1) and insights into ligand binding through molecular docking studies, *International Journal of Molecular Sciences*, **21**(11), 4058.

Muema, F.W., Liu, Y., Zhang, Y., Chen, G., and Guo, M., 2022, Flavonoids from S*elaginella doederleinii* Hieron and their antioxidant and antiproliferative activities, *Antioxidants*, **11**(6), 1189.

O'Leary, C., Gasper, H., Sahin, K.B., Tang, M., Kulasinghe, A., Adams, M.N., *et al.*, 2020, Epidermal growth factor receptor (EGFR)-mutated non-small-cell lung cancer (NSCLC), *Pharmaceuticals*, **13**(10), 273.

Pijuan, J., Barceló, C., Moreno, D.F., Maiques, O., Sisó, P., Marti, R.M., *et al.*, 2019, *In vitro* cell migration, invasion, and adhesion assays: from cell imaging to data analysis, *Frontiers in cell and developmental biology*, **7**, 107.

Prava, J., and Pan, A., 2022, *In silico* analysis of Leishmania proteomes and protein-protein interaction network: Prioritizing therapeutic targets and drugs for repurposing to treat leishmaniasis, *Acta Tropica*, **229**, 106337.

Rajaei, N., Rahgouy, G., Panahi, N., and Razzaghi-Asl, N., 2023, Bioinformatic analysis of highly consumed phytochemicals as P-gp binders to overcome drug-resistance, *Research in Pharmaceutical Sciences*, **18**(5), 505-516.

Ramírez, D., and Caballero, J., 2018, Is it reliable to take the molecular docking top scoring position as the best solution without considering available structural data?, *Molecules*, **23**(5), 1038.

Ramos, A., Sadeghi, S., and Tabatabaeian, H., 2021, Battling chemoresistance in cancer: root causes and strategies to uproot them, *International Journal of Molecular Sciences*, **22**(17), 9451.

Rehman, N., and Qamar, S., 2022, Numerical Approximation of the Nonequilibrium Model of Gradient Elution Chromatography Considering Linear and Nonlinear Solvent Strength Models, *ACS omega*, **7**(36), 31905-31915.

Ren, M., Li, S., Gao, Q., Qiao, L., Cao, Q., Yang, Z., *et al.*, 2023, Advances in the Anti-Tumor Activity of Biflavonoids in Selaginella, *International Journal of Molecular Sciences*, **24**(9), 7731.

Shen, B., Shangguan, X., Yin, Z., Wu, S., Zhang, Q., Peng, W., *et al.*, 2021, Inhibitory effect of fisetin on α-glucosidase activity: Kinetic and molecular docking studies, *Molecules*, **26**(17), 5306.

Shivaleela, B., Srushti, S.C., Shreedevi, S.J., and Babu, R.L., 2022, Thalidomide-based inhibitor for TNF-α: designing and Insilico evaluation, *Future Journal of Pharmaceutical Sciences*, **8**, 1-10.

Sivasakthi, P., Sabarathinam, S., and Vijayakumar, T.M., 2022, Network pharmacology and *in silico* pharmacokinetic prediction of Ozanimod in the management of ulcerative colitis: A computational study, *Health Science*

*Reports*, **5**(1), e473.

Suarez-Arnedo, A., Figueroa, F.T., Clavijo, C., Arbeláez, P., Cruz, J.C., and Muñoz-Camargo, C., 2020, An image J plugin for the high throughput image analysis of *in vitro* scratch wound healing assays, *PloS one*, **15**(7), e0232565.

Susanti, N.M., Saputra, P., and Hendrayati, L.P., 2018, Molecular Docking Sianidin dan Peonidin sebagai Antiinflamasi pada Aterosklerosis Secara *In Silico*, *Jurnal Farmasi Udayana*, **7**(1), 28.

Tamirat, M.Z., Koivu, M., Elenius, K., and Johnson, M.S., 2019, Structural characterization of EGFR exon 19 deletion mutation using molecular dynamics simulation, *PloS one*, **14**(9), e0222814.

Torres, P.H., Sodero, A.C., Jofily, P., and Silva-Jr, F.P., 2019, Key topics in molecular docking for drug design, *International Journal of Molecular Sciences*, **20**(18), 4574.

Varella, L., and Cristofanilli, M., 2023, Evaluating elacestrant in the management of ER-positive, HER2-negative advanced breast cancer: evidence to date, *OncoTargets and Therapy*, **16**, 189-196.

Wang, S., Wan, D., Liu, W., Kang, X., Zhou, X., Sefidkon, F., *et al.*, 2022, A Biflavonoid-Rich Extract from *Selaginella doederleinii* Hieron. against Throat Carcinoma via Akt/Bad and IKKβ/NF-κB/COX-2 Pathways, *Pharmaceuticals*, **15**(12), 1505.

World Health Organization, 2022, February 3, Cancer, Accesed on 5 June 2023 from World Health Organization International: https://www.who.int/news-room/fact-sheets/detail/cancer.

Xu, D., Wang, X., Huang, D., Chen, B., Lin, X., Liu, A., and Huang, J., 2022, Disclosing targets and pharmacological mechanisms of total bioflavonoids extracted from *Selaginella doederleinii* against non-small cell lung cancer by combination of network pharmacology and proteomics, *Journal of Ethnopharmacology*, **286**, 114836.

Zhuang, W.R., Wang, Y., Cui, P.F., Xing, L., Lee, J., Kim, D., *et al.*, 2019, Applications of π-π stacking interactions in the design of drug- delivery systems, *Journal of controlled release*, **294**, 311-326.